

Vortex trimer in three-component Bose-Einstein condensates

Minoru Eto¹ and Muneto Nitta²

¹*Department of Physics, Yamagata University, Yamagata 990-8560, Japan*

²*Department of Physics, and Research and Education Center for Natural Sciences, Keio University, Hiyoshi 4-1-1, Yokohama, Kanagawa 223-8521, Japan*

(Dated: March 13, 2022)

Vortex trimer is predicted in three-component Bose-Einstein condensates (BEC's) with internal coherent couplings. The molecule is made by three constituent vortices which are bounded by domain walls of the relative phases. We show that the shape and the size of the molecule can be controlled by changing the internal coherent couplings.

PACS numbers: 03.75.Lm, 03.75.Mn, 11.25.Uv, 67.85.Fg

I. INTRODUCTION

Recent advances in realizing Bose-Einstein condensates (BEC's) in ultracold atomic gases have opened new possibilities of quantum physics [1, 2]. One of them is interpenetrating superfluids, a mixture of two or more superfluids. Such multicomponent BEC's can be realized when more than one hyperfine spin state is simultaneously populated or when more than one species of atoms are mixed. The *s*-wave scattering wave-length can be tuned via a Feshbach resonance [3–5]. Moreover, recent experimental achievement of a condensate of ytterbium offers condensations up to five components [6]. Stability condition of multicomponent BEC's was studied in Ref. [7]. One of the most important consequences of superfluidity is the existence of vortices. Vortices in multicomponent BEC's have been realized experimentally [8, 9], and structures of those vortices are much richer than those of single components [10–12].

In the case of multiple hyperfine spin states, the internal coherent coupling between multiple components can be introduced by Rabi oscillations. This case is similar to two gap superconductors with Josephson coupling between the two gaps. A sine-Gordon domain wall of a phase difference of two components is allowed [13]. Moreover, an integer vortex is split into two fractional vortices with fractional circulations, and they are connected by a sine-Gordon domain wall with the total configuration being a molecule of two constituent vortices, namely, a vortex dimer [14, 15]. Therefore it is natural to ask whether a molecule made of more than two vortices is possible in some case, or how domain walls connect among them if it is possible.

In this paper we explicitly construct a vortex trimer, namely, a molecule made of three constituent vortices winding around respective three components of BEC's with internal coherent couplings induced by Rabi oscillations. Varying the internal coherent couplings, the shape of the molecule is changed accordingly. We also find a dependence of the size of the vortex trimer on the magnitude of the Rabi frequency.

II. THE GROSS-PITAEVSKII MODEL

We consider three-component BEC's of atoms with equal mass m , described by the condensate wave functions ψ_i ($i = 1, 2, 3$) with the energy functional

$$E = \sum_{i,j} \int d^2x \left(-\frac{\hbar^2}{2m} \psi_i^* \nabla^2 \psi_i \delta_{ij} + \frac{g_{ij}}{2} |\psi_i|^2 |\psi_j|^2 - \mu_i |\psi_i|^2 \delta_{ij} - \omega_{ij} \psi_i^* \psi_j \right), \quad (1)$$

where atom-atom interactions are characterized by the coupling constants $g_{ij} = g_{ji}$, μ_i is a chemical potential, and a symmetric tensor $\omega_{ij} = \omega_{ji}$ ($\omega_{ii} = 0$) stands for the Rabi frequency between the i th and j th components. In this paper, we consider the case with $\mu_1 = \mu_2 = \mu_3 \equiv \mu$, $g_{11} = g_{22} = g_{33} \equiv g$, and $g_{12} = g_{23} = g_{31} \equiv \tilde{g}$ for simplicity, but the general case is straightforward. We also assume $g + 2\tilde{g} > 0$ for the stability of ground states.

In the following, we will separately study two cases: the case with $g \neq \tilde{g}$ ($\det g_{ij} \neq 0$) and the $U(3)$ symmetric case with $g = \tilde{g}$ ($\det g_{ij} = 0$).

Let us first study the former case. When all the Rabi frequencies vanish, the ground state is given by

$$|\psi_i|^2 = v^2, \quad v \equiv \sqrt{\frac{\mu}{g + 2\tilde{g}}}, \quad (i = 1, 2, 3). \quad (2)$$

The topology of the ground state is characterized $\pi_1[U(1)^3] = \mathbb{Z} \oplus \mathbb{Z} \oplus \mathbb{Z}$. Once the small Rabi frequencies are turned on, only the overall $U(1)$ symmetry remains contact and the homotopy group also reduces to $\pi_1[U(1)] = \mathbb{Z}$. At the same time, the magnitudes of the condensates are modified. This is because the Rabi frequencies yield potentials on the relative phases of $\theta_i = \arg \psi_i$. The ground state can be obtained by solving a variational equation $\delta E / \delta \psi_i = 0$. We denote the condensate wave function of the ground state by

$$\psi_i = v_i e^{i\theta_i}, \quad (v_i > 0). \quad (3)$$

The last term in Eq. (1) can be written as $-2v_i v_j \omega_{ij} \cos(\theta_i - \theta_j)$. For $\omega_{ij} > 0$, the phases θ_i and θ_j tend to coincide, $\theta_i = \theta_j$, to reduce this interaction

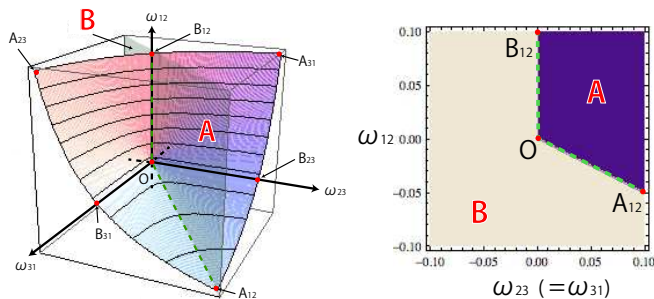


FIG. 1: (Color online) The parameter region where Eq. (4) holds. The left panel shows the boundary surface on which Eq. (4) holds inside (the region A) while it does not hold outside (the region B). The plot range of the left panel is $-0.05 \leq \omega_{ij} \leq 0.1$. The right panel shows the cross section $\omega_{23} = \omega_{31}$. Some points $\{A_{ij}, B_{ij}, O\}$ on the surface are shown: A_{12} is placed at $(\omega_{12}, \omega_{23}, \omega_{31}) = (-0.05, 0.1, 0.1)$, B_{12} is at $(0.1, 0, 0)$, and the other points are obtained by the \mathbb{Z}_3 rotations around O .

energy. Therefore, when $\omega_{ij} > 0$ hold for all $i, j = 1, 2, 3$, all the phases coincide,

$$\theta_1 = \theta_2 = \theta_3, \quad (4)$$

in the ground state. We numerically find that relation (4) is satisfied in the parameter region A shown in Fig. 1. We note that Eq. (4) holds not only when all ω_{ij} 's are positive but also in the region where one of the ω_{ij} 's is negative. In this paper, we consider region A, where relation (4) holds. The other region is frustrated, which will be studied elsewhere.

III. VORTEX CONFIGURATIONS

The nontrivial first homotopy group immediately leads to the existence of superfluid vortices. In particular, the case with $g \neq \tilde{g}$ would have three different kinds of vortices because of the homotopy group $\pi_1[U(1)^3] = \mathbb{Z} \oplus \mathbb{Z} \oplus \mathbb{Z}$ (when $\omega_{ij} = 0$).

Let us consider an integer vortex configuration in which all the condensations ψ_i have unit winding in $U(1)$'s. The asymptotic behavior of such a configuration at large distance from the vortices should be

$$(\psi_1, \psi_2, \psi_3) \rightarrow (v_1 e^{i\theta}, v_2 e^{i\theta}, v_3 e^{i\theta}), \quad (5)$$

which satisfies the ground-state condition (4). Here θ stands for the angular coordinate as $x + iy = re^{i\theta}$. We will show that this vortex is deformed to a vortex trimer made of three constituent vortices, $(v_1 e^{i\theta}, v_2, v_3)$, $(v_1, v_2 e^{i\theta}, v_3)$, and $(v_1, v_2, v_3 e^{i\theta})$, which we call (1,0,0)-, (0,1,0)- and (0,0,1)-vortices, respectively. Since it is a dynamical problem if the constituent vortices make a bound state or not, let us see the two cases $\omega_{ij} = 0$ and $\omega_{ij} \neq 0$ separately.

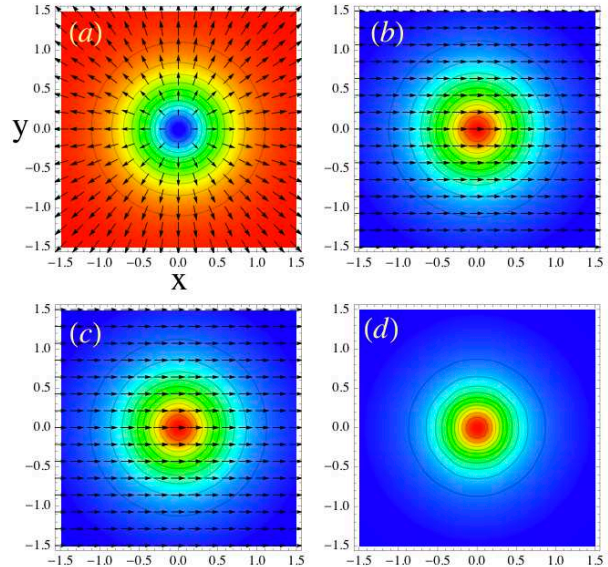


FIG. 2: (Color online) The panels (a), (b), and (c) show the profiles of the density $|\psi_1|^2$, $|\psi_2|^2$, and $|\psi_3|^2$ for the (1,0,0)-vortex in the case where $g \neq \tilde{g}$, respectively. The arrows show a phase vector $(\text{Re}(\psi_i), \text{Im}(\psi_i))$. The energy density is shown in panel (d). We choose $\hbar = m = 1$, $g = 1000$, $\tilde{g} = 900$, $\mu = 100$. The Rabi frequencies are $\omega_{12} = \omega_{23} = \omega_{31} = 0$. The sizes of the boundary are $L = -15$ to $L = 15$ for both x and y .

When the Rabi frequencies vanish ($\omega_{ij} = 0$), the constituent vortices do not make a molecule since they repel each other. Instead, the constituent vortex can exist alone; see Fig. 2, where a numerical solution [18] of the constituent vortex is shown. The tension (energy per unit length) of the constituent vortex is given by $\frac{\pi \hbar^2 v^2}{m} \ln \frac{L}{\xi}$ with system size L and healing length ξ .

On the other hand, when the Rabi frequencies are not zero, the unit constituent vortex alone is unstable because semi-infinite domain walls are attached to it. This domain wall supplies attractive force between the constituent vortices and can be balanced with repulsion among them, so that the constituent vortices form a vortex trimer (vortex dimers are stable only when two of the Rabi frequencies are zero). To understand this better, it is useful to consider a reduced model from Eq. (1) by fixing the amplitudes $|\psi_i| \simeq v_i$ ($v_i \simeq v$ for simplicity). Then we are left with three phases:

$$\Theta = \sum_i \theta_i, \quad \delta_{1,2,3} = \theta_{2,3,1} - \theta_{3,2,1}. \quad (6)$$

The Hamiltonian of the reduced model is given by

$$H = \frac{\hbar^2 v^2}{6m} \left[(\nabla\Theta)^2 + \sum_i ((\nabla\delta_i)^2 - \tilde{\omega}_i \cos \delta_i) \right], \quad (7)$$

where we have introduced the renormalized couplings $\tilde{\omega}_{1,2,3} = \frac{12m}{\hbar^2} \omega_{23,31,12}$. This approximation is valid only when the Rabi frequencies are much smaller than the other coupling constants. [19] For example, let us consider the (1,0,0)-vortex, with relative phases given by

$$\delta_1 = 0, \quad \delta_2 = -\theta_1, \quad \delta_3 = \theta_1. \quad (8)$$

Then the potential term reads

$$V = -\frac{\hbar^2 v^2}{6m} (\tilde{\omega}_2 \cos \delta_2 + \tilde{\omega}_3 \cos \delta_3). \quad (9)$$

When $\tilde{\omega}_{2,3} > 0$, $\delta_2 = \pi$ is an unstable point and a semi-infinite domain wall appears on the negative region of the real axis. Its tension is given by

$$T_1 = \sqrt{T_{12}^2 + T_{31}^2}, \quad T_{ij} = \frac{8\sqrt{6}}{3} \frac{\mu\hbar\sqrt{\omega_{ij}}}{\sqrt{m}(g+2\tilde{g})}. \quad (10)$$

This is the origin of the attractive force between the constituent vortices. Note that, since we have two relative phases δ_2 and δ_3 , one may naturally imagine two independent domain walls. Each domain wall has the tension T_{31} (when we set $\omega_{12} = 0$) and T_{12} (when we set $\omega_{31} = 0$). However, for the (1,0,0)-vortex, the two relative phases are related as $\delta_2 = -\delta_3$ and these two domain walls stick together and form a bound state. Indeed, the total tension T_1 is the square root of the sum of T_{12}^2 and T_{31}^2 as shown in Eq. (10), which is smaller than the sum of the two tensions, $T_1 \leq T_{12} + T_{31}$.

IV. NUMERICAL SOLUTIONS OF VORTEX TRIMERS

We have numerically found stable vortex trimers as unique solutions under the boundary condition (5) in a wide range of the parameter region A in Fig. 1. Here in Fig. 3 we show several numerical solutions as examples with $g = 1000$ and $\tilde{g} = 900$ ($\mu = 100$ and $m = \hbar = 1$). The rightmost panels show the energy density in which the partonic structure is clearly seen. The contours therein show contributions from the last term of Eq. (1). Since the distance between the constituent vortices are close, we cannot see domain walls. Nevertheless, qualitative estimation from the reduced model is quite useful, as will be seen below.

Each line of Fig. 3 gives a molecule with different Rabi frequencies. First of all, the fourth line of Fig. 3 shows a \mathbb{Z}_3 symmetric trimer where the Rabi frequencies are all equal as $\omega_{12} = \omega_{23} = \omega_{31} = 0.05$. One can see that the phases at the spatial infinity are indeed aligned ($\theta_1 = \theta_2 = \theta_3$). Next, by changing ω_{12} from the symmetric case, we can observe how the shape of the trimer

is deformed. Since the Rabi frequency ω_{12} controls the interaction between the (1,0,0)- and the (0,1,0)-vortices, the equilateral triangle is deformed to an isosceles triangle. The third line of Fig. 3 shows the vortex trimers with $\omega_{12} = 0.01$, in which the attractive force between the (1,0,0)- and the (0,1,0)-vortices is smaller than those between the other two pairs. Therefore the internal angle at the vertex at the (0,0,1)-vortex is larger than $\pi/3$. We also show the vortex trimer when $\omega_{12} = 0$ in the second line of Fig. 3. Since no attractive force exists between the (1,0,0)- and the (0,1,0)-vortices, the shape of the molecule becomes a stick as expected. We also find the molecule even when ω_{12} is negative ($= -0.01$) while $\omega_{23} = \omega_{31} = 0.05$; see the first line of Fig. 3. We still observe a stick-type molecule whose length is slightly larger than that for $\omega_{12} = 0$. In the last two lines of Fig. 3, we have chosen $\omega_{12} = 0.2$ and 0.5 , which are larger than $\omega_{23} = \omega_{31} = 0.05$ (the \mathbb{Z}_3 -symmetric case). Since the attractive force between the (1,0,0)- and the (0,1,0)-vortices is stronger than those for the other two pairs, we see that the corresponding edge of the triangle becomes shorter than the other two edges. Since $\omega_{12} = 0.5$ yields an attractive force that is too strong, the triangle collapses, as shown in the last line of Fig. 3.

We have seen that the shape of the triangle changes according to the choice of the Rabi frequencies. Here, we investigate a correlation of the Rabi frequencies, set to be equal $\omega_{12} = \omega_{23} = \omega_{31} \equiv \omega$, and the size of the equilateral triangle, see Fig. 4. We numerically find the relation

$$A \simeq 0.56 \omega^{-0.25}, \quad (11)$$

for the range $0.01 \leq \omega \leq 0.1$, where A stands for the length of the edge of the equilateral triangle.

Let us finally consider a vortex trimer in the $U(3)$ symmetric case ($g = \tilde{g}$) where all of the terms in Eq. (1) except for the last one are invariant under $\vec{\psi} \rightarrow U\vec{\psi}$ with $U \in U(3)$. A striking difference from the previous case with $g \neq \tilde{g}$ can be best seen in the limit where $\omega_{ij} \rightarrow 0$. The ground state is degenerate and its order parameter space is $U(3)/U(2) \simeq S^5$ defined by $\sum_{i=1}^3 |\psi_i|^2 = \frac{\mu}{g}$. The first homotopy group of the ground state is trivial, and there are no topologically stable vortices. When the Rabi frequencies are not zero, the order parameter space becomes $U(1)$ implying the existence of stable vortex configuration. Fig. 5 shows numerical solutions for several choice of the Rabi frequencies. We examine two choices for the Rabi frequencies with $g = \tilde{g} = 1000$ ($\mu = 100$ and $\hbar = m = 1$): i) $\omega_{12} = \omega_{23} = \omega_{31} = 0.1$, which leads to the ground state condensation $(|\psi_1|, |\psi_2|, |\psi_3|) = (0.183, 0.183, 0.183)$, and ii) $\omega_{23} = 0.05$, $\omega_{12} = \omega_{31} = 0.1$, which leads to $(|\psi_1|, |\psi_2|, |\psi_3|) = (0.203, 0.171, 0.171)$. Although the profiles of the condensation are not axisymmetric, the total energy density is universally axisymmetric; see the rightmost panels in Fig. 5. Unlike the previous case with $g \neq \tilde{g}$, it is impossible to see a partonic nature from the energy density when $g = \tilde{g}$. These things are related to the fact that there are no con-

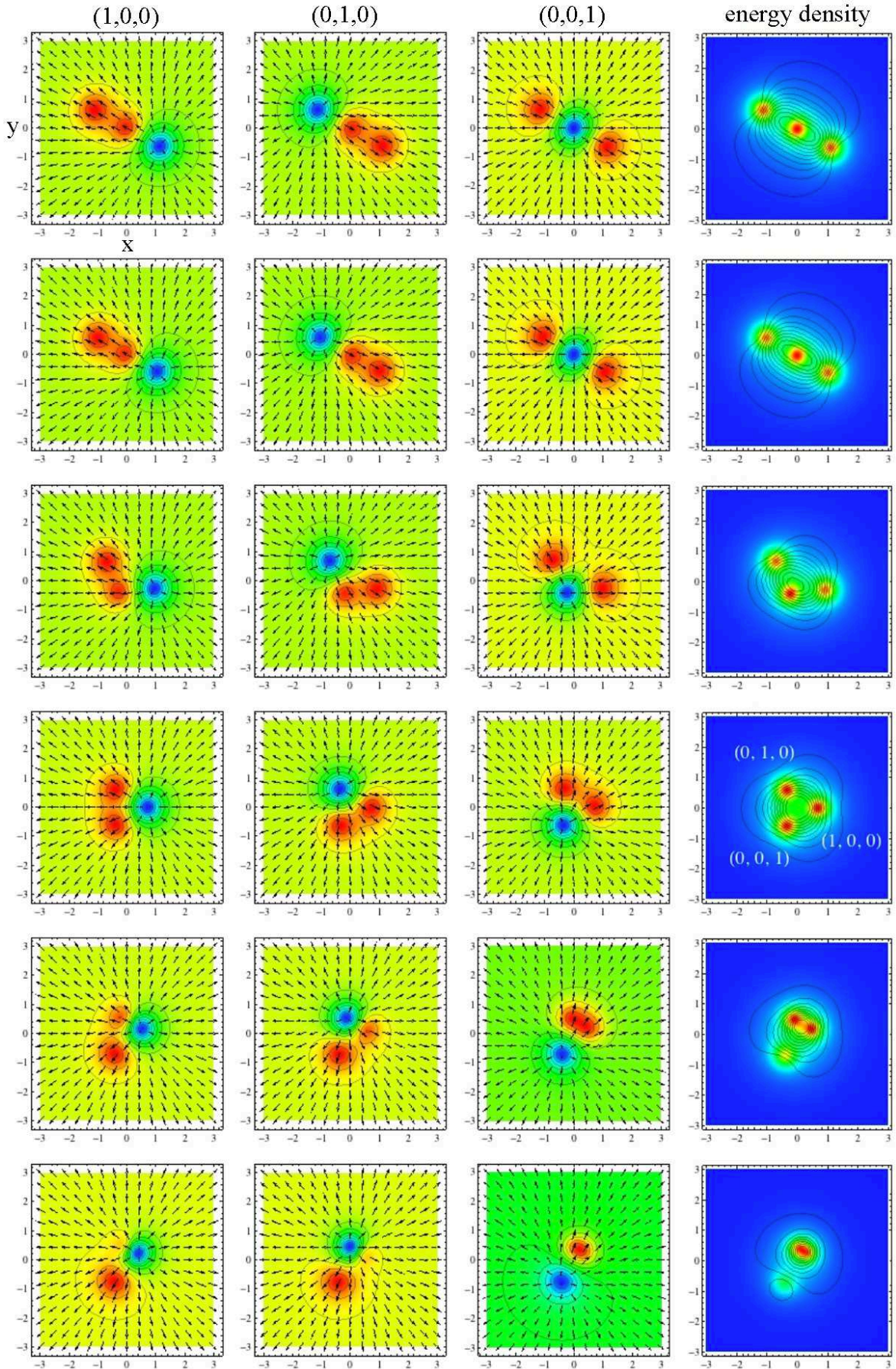


FIG. 3: (Color online) The left three panels show the profiles of the density $|\psi_i|^2$ and the phases ($\text{Re}[\psi_i]$, $\text{Im}[\psi_i]$) for the unit vortex trimer in the case $g \neq \tilde{g}$, respectively. The rightmost panel shows the energy density and the contour corresponds to the Rabi potential. The constants are taken as $\hbar = m = 1$, $\mu = 100$, $g = 1000$, $\tilde{g} = 900$, and $\omega_{23} = \omega_{31} = 0.05$. We change the Rabi frequency ω_{12} from the top to the bottom as $\omega_{12} = -0.01, 0, 0.01, 0.05, 0.2, 0.5$, respectively. The sizes of the boundary are $L = -8$ to $L = 8$ for both x and y .

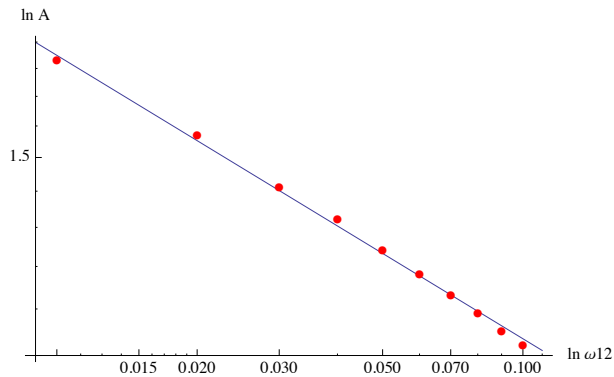


FIG. 4: (Color online) Loglog-plot of $|\omega_{12}|$ vs the length (A) of an edge of the equilateral triangle with $\omega_{12} = \omega_{23} = \omega_{31}$. The corresponding configuration is given in the fourth line of Fig. 3. The parameters are fixed as $\hbar = m = 1$, $\mu = 100$ and $g = 1000$ and $\tilde{g} = 900$.

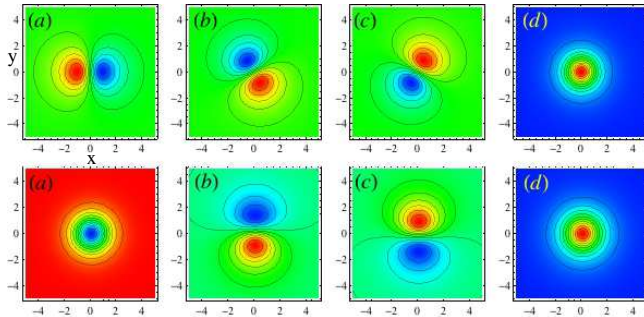


FIG. 5: (Color online) The panels (a), (b), and (c) show the profiles of the density $|\psi_1|^2$, $|\psi_2|^2$, and $|\psi_3|^2$ for the minimal vortex in the $U(3)$ -symmetric case, respectively. The energy density is shown in panel (d). We choose $\hbar = m = 1$, $g = \tilde{g} = 1000$, $\mu = 100$. The Rabi frequencies are chosen as $\omega_{12} = \omega_{23} = \omega_{31} = 0.1$ in the first row, and $\omega_{23} = 0.05$, $\omega_{12} = \omega_{31} = 0.1$ in the second row. The sizes of the boundary are $L = -15$ to $L = 15$ for both x and y .

stituent vortices standing alone in the limit $\omega_{ij} \rightarrow 0$. This configuration can be regarded as a skyrmion in the $\mathbb{C}P^2$ nonlinear sigma model with the two-dimensional complex

projective space $\mathbb{C}P^2 \simeq S^5/S^1 \simeq SU(3)/[SU(2) \times U(1)]$, instead of $\mathbb{C}P^1 \simeq S^3/S^1 \simeq SU(2)/U(1) \simeq S^2$ for two component BECs [14].

V. DISCUSSION

Finally, we comment on the possibility of realization in experiments. In this paper, we have solved the GP equation in the static system by fixing the phase winding and the constant density at the boundaries [18]. This implies that the vortex trimer is created in rotating BECs in laboratory experiments. First, an integer vortex is created as usual by gradually increasing the rotation, and then it will be split into the vortex trimer. Two component BEC's of different hyperfine states of the same atom have been already realized using the $|1, -1\rangle$ and $|2, 1\rangle$ states [8] and the $|2, 1\rangle$ and $|2, 2\rangle$ states [16] of ^{87}Rb , respectively. Three component system should be possible using a mixture of those states of ^{87}Rb . For that, one needs to use the optical trap which has been recently been realized in a two-component system [17].

In this paper, we have investigated the vortex trimer in the three-component BEC's. We expect that the vortex N -omers can also be constructed in N -component BEC's. However, for $N \geq 4$, the choice of the internal coherent couplings ω_{ij} becomes nontrivial. For instance, for $N = 4$, we expect that the choice $\omega_{12} = \omega_{23} = \omega_{34} = \omega_{41} > 0$ gives a symmetric tetramer, but we still have additional parameters ω_{13} and ω_{24} . We will study the N -omer elsewhere.

Acknowledgments

We would like to thank K. Kasamatsu and S. Tojo for useful comments. This work is supported in part by Grant-in Aid for Scientific Research (No. 23740198 and No. 23740226) and by the ‘‘Topological Quantum Phenomena’’ Grant-in Aid for Scientific Research on Innovative Areas (No. 23103515) from the Ministry of Education, Culture, Sports, Science and Technology (MEXT) of Japan.

[1] C. J. Pethick and H. Smith, *Bose-Einstein Condensation in Dilute Gases*, 2nd ed. (Cambridge University Press, New York, 2008).
 [2] M. Ueda, *Fundamental and New Frontiers of Bose-Einstein Condensation*, (World Scientific, 2010)
 [3] G. Thalhammer, G. Barontini, L. De Sarlo, J. Catani, F. Minardi, and M. Inguscio, Phys. Rev. Lett. **100**, 210402 (2008).
 [4] S. B. Papp, J. M. Pino, and C. E. Wieman, Phys. Rev. Lett. **101**, 040402 (2008).
 [5] S. Tojo, Y. Taguchi, Y. Masuyama, T. Hayashi, H. Saito,

and T. Hirano, Phys. Rev. A **82**, 033609 (2010).
 [6] T. Fukuhara, S. Sugawa and Y. Takahashi, Phys. Rev. A **76**, 051604(R) (2007).
 [7] D. C. Roberts and M. Ueda, Phys. Rev. A **73**, 053611 (2006).
 [8] M. R. Matthews, B. P. Anderson, P. C. Haljan, D. S. Hall, C. E. Wieman, and E. A. Cornell, Phys. Rev. Lett., **83**, 2498 (1999).
 [9] V. Schweikhard, I. Coddington, P. Engels, S. Tung, and E. A. Cornell Phys. Rev. Lett. **93**, 210403 (2004).
 [10] K. Kasamatsu, M. Tsubota and M. Ueda, Int. J. Mod.

- Phys. B **19**, 1835 (2005).
- [11] M. Eto, K. Kasamatsu, M. Nitta, H. Takeuchi and M. Tsubota, Phys. Rev. A **83**, 063603 (2011).
- [12] P. Mason and A. Aftalion, Phys. Rev. A **84**, 033611 (2011).
- [13] D. T. Son, M. A. Stephanov, Phys. Rev. **A65**, 063621 (2002). [cond-mat/0103451].
- [14] K. Kasamatsu, M. Tsubota and M. Ueda, Phys. Rev. Lett. **93**, 250406 (2004).
- [15] Vortex molecules of a different type are also studied in a spinor BEC, A. M. Turner and E. Demler, Phys. Rev. **B 79**, 214522 (2009).
- [16] P. Maddaloni, M. Modugno, C. Fort, F. Minardi, and M. Inguscio, Phys. Rev. Lett. **85**, 2413 (2000)
- [17] C. Hamner, J. J. Chang, P. Engels, and M. A. Hoefer, Phys. Rev. Lett. **106**, 065302 (2011).
- [18] We use the relaxation (the imaginary time) method for the numerical computation in this paper. We choose the boundary condition with the fixed phase winding and the constant density as given in Eq. (5).
- [19] This condition meets our purpose, since we would not like to consider too large Rabi frequencies such that the size of the molecule given in Eq. (11) becomes comparable to the healing length of the system. In this case, the vortex trimer cannot be distinguished from an integer vortex.